Crystal structure, thermal behavior and vibrational studies of tetraethylammonium dihydrogenarsenate *bis*-arsenic acid [(C$_2$H$_5$)$_4$N].[H$_2$AsO$_4$].[H$_3$AsO$_4$]$_2$

Ikram Dhouib [a],*, Philippe Guionneau [b], Tahar Mhiri [a] and Zakaria Elaoud [a]

[a] Laboratoire de Physico-Chimie de l'Etat Solide, Département de Chimie, Faculté des Sciences de Sfax, Université de Sfax, Sfax 3000, Tunisia
[b] CNRS, Université de Bordeaux, ICMCB, 87 avenue du Dr A. Schweitzer, Pessac, F-33608, France

*Corresponding author at: Laboratoire de Physico-Chimie de l'Etat Solide, Département de Chimie, Faculté des Sciences de Sfax, Université de Sfax, Sfax 3000, Tunisia.
Tel.: +2.169.7019206. Fax: +2.167.4274437. E-mail address: ikramdhouib82@yahoo.fr (I. Dhouib).

ARTICLE INFORMATION

ABSTRACT

An organic-inorganic hybrid compound of tetraethylammonium dihydrogenarsenate *bis*-arsenic acid salts of formula [(CH$_3$CH$_2$)$_4$N].[H$_2$AsO$_4$].[H$_3$AsO$_4$]$_2$ (TEAs) were grown by the slow evaporation and characterized by means of single crystal X-ray diffraction, thermal analysis, FT-IR and Raman spectroscopy. This compound crystallize in the space groups *Cc* with unit cell parameters, a = 20.105(2) Å; b = 7.342(4) Å, c = 15.292(2) Å, γ = 115(4)°, Z = 4, R = 0.07. The structure has solved using direct methods and refined by least-squares analysis. In this case, the structure consists of infinite parallel two-dimensional planes built of mutually H$_2$AsO$_4^-$, H$_3$AsO$_4$ tetrahedra connected by strong O-H···O hydrogen bonding. The thermoanalytical properties were studied using TG of TEAs method in the temperature ranges from 300 to 440 K for this hygroscopic sample. DSC measurement was carried out in the temperature range from 305 to 425 K.

1. Introduction

The combination of organic molecules and inorganic materials was the starting point for the development of new hybrid compounds, with desired physical and chemical properties [1,2]. These compounds have attracted great attention because of their unique opportunity to combine the remarkable features of organic compounds with those of inorganic materials. Their applications have been explored and reported in various fields, such as electronic [3,4], optical [5,6] magnetic [7,8] and ferroelectric [9,10].

In organic-cation monophosphate/monoarsenate, the phosphate/arsenate anions are interconnected by strong hydrogen bonds so as to build infinite networks with various geometries: ribbons [11], chains [12,13], two-dimensional network [14,15], and three-dimensional network [16].

On the other hand, there is still growing interest in the study of crystal containing tetra-alkylammonium cations of the general formula (C$_n$H$_{2n+1}$)$_4$N$^+$ such as (CH$_3$)$_4$N$^+$, (C$_2$H$_5$)$_4$N$^+$ and (C$_3$H$_7$)$_4$N$^+$. The specific geometry of these cations can generate supramolecular networks in one, two or three dimensions. Recently, numerous tetra-ethylammonium derivatives structural and vibrational studies have been published [17-18].

However, in conjunction with some resent works on these hybrids compounds, the crystal structure and vibrational studies of many organic-inorganic crystals have been investigated in our laboratory [19-21]. The present work deals with the growth, single crystal X-ray diffraction (XRD) study, thermal analysis and the detailed vibrational spectral analysis of a new organic-inorganic: tetraetylammonium dihydrogen monoarsenate *bis*-arsenic acid (TEAs).

2. Experimental

2.1. Synthesis

The crystal of the title compound, TEAs, is prepared by slow evaporation at room temperature of an aqueous solution of arsenic acid H$_3$AsO$_4$, and tetraethylammonium hydroxide [CH$_3$CH$_2$]$_4$NOH in the stoichiometric ratio (3:1) and mixed well using a magnetic stirrer to ensure homogenous concentration in the entire volume of the solution. The solutions which allowed evaporating at room temperature a few days until colorless parallel piped shaped monocrystals of TEAs were formed. The reaction scheme involved in the formation of complex compound is given in (1).
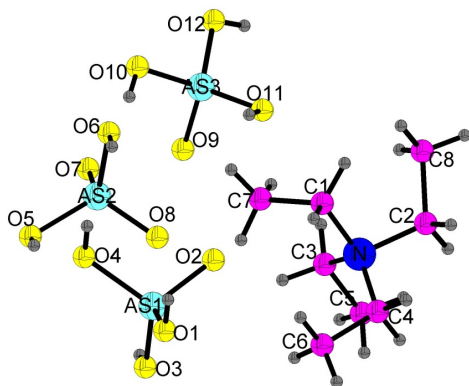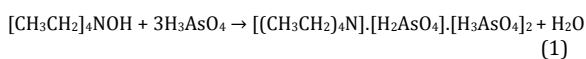
Figure 1. The asymmetric unit of $[(CH_3CH_2)_4N]$ (H_2AsO_4) $(H_3AsO_4)_2$.

$$[CH_3CH_2]_4NOH + 3H_3AsO_4 \rightarrow [(CH_3CH_2)_4N].[H_2AsO_4].[H_3AsO_4]_2 + H_2O \quad (1)$$

2.2. X-ray single crystal structure determination

The structure of TEAs was determined by the X-ray single crystal diffraction method. In each case, a suitable crystal was selected under a polarizing microscope and mounted on a thin glass fiber. The unit cell dimensions of salt was measured and refined using indexation of diffraction markings collected with a Kappa CAD4 automated four-circle diffractometer (graphite-monochromated MoKα radiation, λ = 0.71073 Å). Peak search, centering, indexing and least squares refinement routines led to a monoclinic unit cell for the compound. The final unit cell constants were determined by a least-squares fit of 5066 reflections. The crystal structure was solved by direct methods using SHELXS-97 [22] and difference Fourier synthesis. All the hydrogen positions were geometrically and affined located.

2.3. Spectroscopic measurements

The Fourier transform infrared (FT-IR) spectrum of TEAs was recorded in the range 4000-400 cm^{-1}, with samples in KBr pellets using Perkin-Elmer FT-IR spectrometer. The resolution of the spectrum is ±2 cm^{-1}. The Fourier transform Raman (FT-Raman) spectrum of the same compound was recorded using Horiba Jobin Yvon LabRAM HR 800 Dual spectrophotometer. The incident laser excitation is 632 nm. The scattered light was collected at the angle of 180 ° in the region 3600-50 cm^{-1} and the resolution was set up to 2 cm^{-1}.

3. Results and discussion

3.1. Structural analysis of TEAs

The crystals of the title compound belong to the centrosymmetric Cc space group of the monoclinic system, with $Z = 4$. The lattice parameters are listed in Table 1. The bond lengths and angles are collected in Table 2.

The asymmetric unit is composed of one $[H_2AsO_4]^-$ anion, two neutral arsenic acid $[H_3AsO_4]$ and one $[(CH_3CH_2)_4N]^+$ cation (Figure 1). The structure consists of infinite parallel two-dimensional planes built of mutually $[H_2AsO_4]^-$, $[H_3AsO_4]$ tetrahedra and $(CH_3CH_2)_4N^+$ cations, the projection along the b axis of the atomic arrangement is depicted in Figure 2.

The coordination of arsenic atoms is tetrahedral with As-O distances and O-As-O angles in the ranges (1.622(13); 1.796(7) Å); (1.556(14); 1.739(10)Å); (1.634(10); 1.718(8)Å); (107.7(5); 113.5(6)°); (103.1(6); 114.8(6)°) and (103.0(5); 115.8(5)°) for $[H_3As(1)O_4]$; $[H_2As(2)O_4]^-$ and $[H_3As(3)O_4]$, respectively. The calculated average values of the distortion

indices [23] corresponding to the different distances and angles in $[AsO_4]$ tetrahedral $DI(As(1)O) = 0.0290$, $DI(As(2)O) = 0.0384$, $DI(As(3)O) = 0.0162$, $DI(OAs(1)O) = 0.0197$, $DI(OAs(2)O) = 0.0245$, $DI(OAs(3)O) = 0.0326$, $DI(OO) = 0.0167$, $DI(OO) = 0.0123$ and $DI(OO) = 0.0155$ show a high distortion of the (OO) distances of $[H_3As(1)O_4]$; $[H_2As(2)O_4]^{2-}$ and $[H_3As(3)O_4]$, respectively.

Table 1. Crystal data and summary of intensity data collection and structure refinement of TEAs.

Parameter	TEAs
Formula	$C_8H_{28}NAs_3O_{12}$
Temperature (K)	293.0(2)
Wavelength MoKα (A°)	0.71073
Crystal system	Monoclinic
Space group	*Cc*
Unit cell dimensions	
a (Å)	20.105(5)
b (Å)	7.842(2)
c (Å)	15.292(2)
β (°)	115.00 (2)
Z	4
Calculated density, (g/cm³)	1.53
F(000)	999.8
Crystal size (mm)	0.40 × 0.20 × 0.10
θ range for data collection (°)	2.8-27.1
Index ranges	-25 ≤ *h* ≤ 25
	-9 ≤ *k* ≤ 1
	-19 ≤ *l* ≤ 19
R_{int}	0.0290
R$_{(sigma)}$	0.0395
$R = \sum ||F_o|-|F_c||/\sum ||F_o||$	0.071
R_w	0.2200
T min	0.2604
T max	0.5745
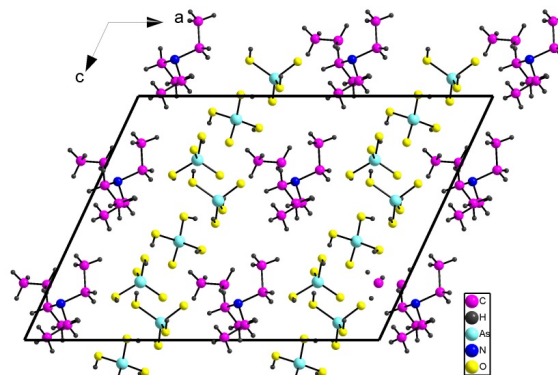
Figure 2. Projection along the *b* axis of the atomic arrangement of $[(CH_3CH_2)_4N].[H_2AsO_4].[H_3AsO_4]_2$.

The structure is based on sheets of $H_2AsO_4^-$ and H_3AsO_4 tetrahedra bonded together by strong intra-layer O-H···O hydrogen bonds, giving to trimmers built up by $[(H_3AsO_4)(H_2AsO_4)]^-$ clusters, (dO−O < 2.73 Å) [24,25] as seen in Figure 3. The mid-planes of these arsenic groups, are located at $x = 0.25$ and $x = 0.75$.

These hydrogen bonds contribute to the cohesion of the structure. The various hydrogen bond parameters are summarized in Table 3.

The organic cation are located at $x = 0.0$ and $x = 0.5$. The lengths of the N-C bonds are in the range between 1.462(17) to 1.600(2) Å. The C-N-C angles range from 101.6(10) to 115.9(12)°. The C-C bonds lengths are in the region between 1.477(13) to 1.611(14) Å. They are in good agreement with those found in related compound [19,21].

3.2. Vibrational analysis

The FT-IR and FT-Raman spectra of the title crystals were measured for the powder sample at room temperature.

Table 2. Principal interatomic distances (Å) and angles (°) in TEAs.

Tetrahedron around As	Distances (Å)	$[CH_3CH_2]_4N^+$ cations	Angles (°)
As(1)-O(1)	1.671(12)	N-C(1)	1.60(2)
As(1)-O(2)	1.622(13)	N-C(2)	1.571(14)
As(1)-O(3)	1.663(14)	N-C(3)	1.470(14)
As(1)-O(4)	1.796(7)	N-C (4)	1.462(17)
O(1)-H(11)	0.8200	C(1)-C(7)	1.580(15)
O(4)-H(14)	0.8200	C(2)-C(8)	1.611(14)
O(3)-H(13)	0.8200	C(3)-C(5	1.556(13)
As(2)-O(5)	1.731(9)	C(4)-C(6)	1.4777 (3)
As(2)-O(6)	1.739(10)	C(1)-N-C(4)	114.2(12)
As(2)-O(7)	1.657(9)	C(1)-N-C(2)	104.9(11)
As(2)-O(8	1.556(14)	C(4)-N-C(2)	101.6(10)
O(5)-H(22)	0.8200	C(1)-N-C(3)	108.8(12)
O(6)-H(23)	0.8200	C(4)-N-C(3)	115.9(12)
As(3)-O(9)	1.634(10)	C(2)-N-C(3)	110.7(12)
As(3)-O(10)	1.718(8)	C(8)-C(2)-N	114.1(12)
As(3)-O(11)	1.704(7)	C(6)-C(4)-N	112.7(6)
As(3)-O(12)	1.698(11)	C(5)-C(3)-N	108.7(10)
O(10)-H(33)	0.8200	C(1)-C(7)-N	98.1(9)
O(11)-H(34)	0.8200		
O(12)-H(31)	0.8200		
O(2)-As(1)-O(4)	107.7(5)		
O(2)-As(1)-O(1)	107.7(5)		
O(4)-As(1)-O(1)	113.5(6)		
O(4)-As(1)-O(3)	108.6(5)		
O(1)-As(1)-O(3)	109.4(6)		
O(2)-As(1)-O(3)	113.0(6)		
O(6)-As(2)-O(5)	107.6(6)		
O(6)-As(2)-O(7)	109.7(5)		
O(5)-As(2)-O(7)	110.6(5)		
O(6)-As(2)-O(8)	103.1(6)		
O(5)-As(2)-O(8)	110.5(6)		
O(7)-As(2)-O(8)	114.8(6)		
O(11)-As(3)-O(10)	108.6(4)		
O(11)-As(3)-O(9)	106.2(5)		
O(10)-As(3)-O(9)	109.2(5)		
O(11)-As(3)-O(12)	115.8(5)		
O(10)-As(3)-O(12)	103.0(5)		
O(9)-As(3)-O(12)	113.8(3)		

Table 3. Bond lengths (Å) and bond angles (°) in the hydrogen bonding scheme of $[(CH_3CH_2)_4N].[H_2AsO_4].[H_3AsO_4]_2$.

D-H···A	d(D-H) (Å)	d(H···A) (Å)	d(D···A) (Å)	∠ D-H···A (°)
O(3)-H(13)···O(12) [i]	0.82	2.04	2.669(15)	132.7
O(4)-H(14) ···O(7)	0.82	1.80	2.614(13)	169.4
O(5)-H(22) ···O(12) [iv]	0.82	2.25	2.560(13)	102.5
O(6)-H(23) ···O(9) [ii]	0.82	1.86	2.453(16)	128.7
O(10)-H(33) ···O(7)	0.82	1.82	2.581(13)	154.3
O(12)-H(31) ···O(3) [iii]	0.82	1.87	2.669(15)	165.3

Symmetry codes: (i) x, $-y+1$, $z+1/2$; (ii) x, $y-1$, z; (iii) x, $-y+1$, $z-1/2$; (iv) x, $-y$, $z+1/2$.
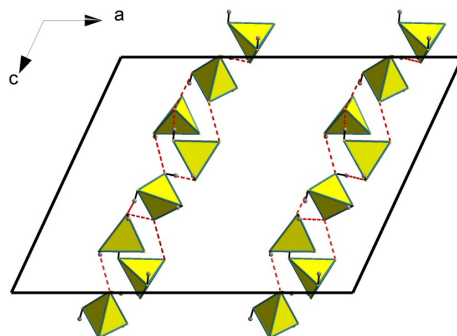
Figure 3. Projection along the *b* axis of the inorganic arrangement of TEAs.

The bands observed in the measured region arise from the vibrations of hydrogen bonds, vibrations of the tetraethyl ammonium cation, arsenic, groups and lattice vibrations. Vibrational spectra are shown in Figure 4-5.

The vibrational analysis of an isolated arsenate, phosphate anion AsO_4^{3-}, with T_d point group symmetry leads to four Raman active normal modes: $\nu_1(A_1)$, $\nu_2(E)$, $\nu_3(F_2)$ and $\nu_3(F_2)$ with average wavenumbers 837, 349, 887 and 463 cm^{-1},

respectively [26]. ν_1 and ν_3 involve the symmetric and the anti-symmetric stretching mode of the As-O bonds, whereas ν_2 involve mainly O-As-O, symmetric and anti-symmetric bending modes. The IR and Raman spectra of TEAs, that we obtained consist of a number of distinct and well separated groups of bands, and can be divided into three frequency regions: 15-250 cm^{-1}, lattice mode; 250-1200 cm^{-1}, AsO_4^{3-}, internal modes and 1200-3700 cm^{-1}, high-frequency hydrogen modes [27-29]. In

TEAs crystal, the symmetry of AsO_4^{3-}, ions is reduced from T_d to C_1. In fact, our structural study on TEAs shows that the As-O, distances and the O-As-O, angles are distorted with respect to the hypothetical T_d symmetry. This symmetry change partially removes the degeneracy of the vibrational wave functions, which would have characterized free AsO_4^{3-}. In the 1000-300 cm^{-1} region, the AsO_4^{3-} stretching and bending vibrations expected to appear, as well as the modes associated to internal modes of the organic cations. However, in the light of our present calculations as primary source of assignment and by comparison with similar organic arsenic compound, we have been distinguishing between the bands originating from the vibrations of arsenate groups and the organic cations. The medium band at 907 cm^{-1} in Raman spectrum is assigned to the asymmetric stretching ν_3 mode of the arsenate ion. In IR spectrum, this mode appears also as a single strong band at 920 cm^{-1}. The band due to the symmetric stretching mode ν_1 vibration is located in Raman spectrum at 829 and 671 cm^{-1} as a strong band. In IR spectrum this mode appears as a strong band at 822 and 677 cm^{-1}. The bands due to the symmetric and asymmetric bending vibration ν_2 and ν_4 of the arsenate ion are identified in the 550-400 cm^{-1} and 400-300 cm^{-1} frequency region, respectively. The very strong band observed in Raman spectrum at 417 cm^{-1} can be easily assigned to ν_4 mode, whereas the symmetric mode ν_2 appears in Raman spectrum as weak band at 324 cm^{-1}.
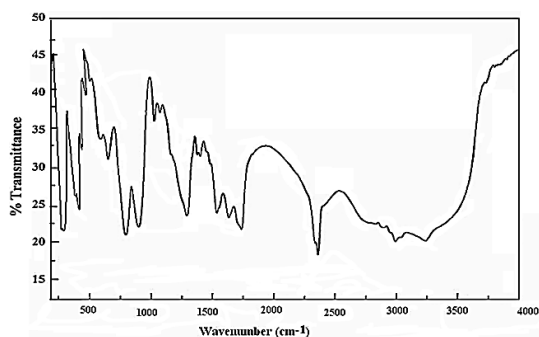

Figure 4. IR spectrum of $[(CH_3CH_2)_4]N \ (H_2AsO_4) \ (H_3AsO_4)_2$.
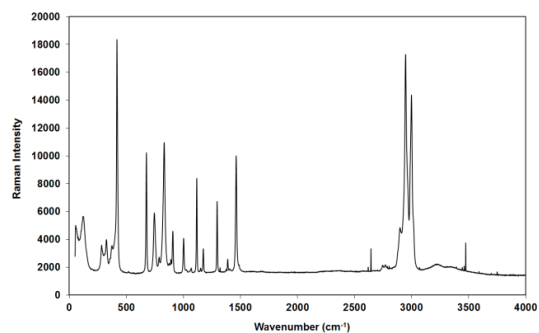
Figure 5. Raman spectrum of $[(CH_3CH_2)_4]N \ (H_2AsO_4) \ (H_3AsO_4)_2$.

Numerous functional and skeletal groups such as CH_2, CH_3, C-N, C-C and NC_4 are present in tetrapropylammonium cation. These groups are manifested in IR and Raman spectra in different range with different intensity.

It is well known that CH_3 groups have C_{3v} symmetry in the free state with pyramidal structure of TEAs. Their normal modes of vibrations are $\nu_1(A_1)$, $\nu_2(A_1)$, $\nu_3(E)$ and $\nu_4(E)$. All these modes are both infrared and Raman active with the asymmetric stretching and bending modes being doubly degenerate. The asymmetric and symmetric CH_3 stretching vibrations in aliphatic compound are usually observed in the region 2990-

2850 cm^{-1} [30-31]. In the title compound the doubly degenerate asymmetric stretching and bending modes $\nu_3(E)$ and $\nu_4(E)$ are observed in the split form. The weak band at 2944 cm^{-1} and the shoulder one at 2948 cm^{-1} in IR spectrum are attributed to the asymmetric stretching vibration and the Raman counterparts are located as a very strong band at 2997 cm^{-1}. The symmetric stretching mode of CH_3 is assigned to the shoulder band at 2897 cm^{-1} in Raman spectrum. In IR spectrum this mode appears as a very weak intensity band at the 2848 cm^{-1}. The asymmetric and symmetric bending mode of methyl group generally appears in the region 1550-1410 and 1310-1400 cm^{-1}, [32-33]. In the present case, two FT-IR bands with slightly different intensity at 1447 and 1478 cm^{-1} are assigned to CH_3 asymmetric bending mode. In Raman spectrum, their corresponding bands appear as a very shoulder band at 1452 cm^{-1} and as a very strong one at 1462 cm^{-1}. The symmetric bending mode of the CH_3 group is seen at 1392 cm^{-1} as a medium band in the IR spectrum and as a very strong band at 1385 cm^{-1} in Raman spectrum. The methyl rocking vibration is observed as a weak band at 997 cm^{-1} in IR spectrum and at 1001 cm^{-1} as a medium one in Raman spectrum.

The wavenumber of the CH_2 vibrational modes depend on its immediate environment. The stretching modes of the CH_2 group usually occur in the region 3100-2800 cm^{-1} [34-35]. In TEAs crystal, the CH_2 asymmetric and symmetric stretching modes are not identified in IR spectrum. These bands are probably masked by the broad bands of CH_3 stretching vibrations. The weak band located at 2874 cm^{-1} in Raman spectrum is assigned to the CH_2 symmetric stretching mode. The deformation modes of this group lie in the same region as the deformation modes of CH_3. Since the deformation modes of methyl group are intense, the deformation modes of CH_2 are also not identified. However the wagging, twisting and the rocking modes of the CH_2 group were observed and assigned.

The primitive unit cell of the title compound contains one tetraethylammonium $(NC_4)^+$ cation not coupled with the inorganic parts as revealed by the X-Ray diffraction. Then, it is convenient as a first approach to consider the NC_4 core of the isolated cation with Td symmetry and therefore exhibits four normal modes. According to the literature, the vibrations related to NC_4 group shown in tetraethylammonium cation of TEAs are described as: symmetric stretching mode $\nu_1(A)$ to be found at 752 cm^{-1}, [36-38] asymmetric stretching mode $\nu_3(F_2)$ located at 955 cm^{-1}, asymmetric bending mode $\nu_4(F_2)$ observed at 455 cm^{-1} and the symmetric bending mode $\nu_2(F_2)$ at 372 cm^{-1} [32,39]. In our case the weak band appeared at 1001, 1000 cm^{-1} is related to the ν_3 mode. His counterpart appears in IR spectrum as shoulder band at 988 cm^{-1}. The weak band observed in Raman spectrum at 744 cm^{-1} arises from the ν_1 symmetric stretching mode. The bands assigned to the symmetric and asymmetric bending modes of NC_4 core of the isolated cation are observed in Raman spectrum at 383 cm^{-1} respectively whereas the corresponding calculated values for these modes are located at 393 cm^{-1}, respectively. It is interest to note that the vibrational mode of the NC_4 group do not deviate much from their expected values, suggesting that the interaction of this group with the environment is not strong on the other hand, we note also that our assignment of NC_4 agree well with the previous reported vibrational studies of the tetraethylammonium salts [40].

It is well known that hydrogen bonding brings a remarkable downward wavenumber shifts. The intermolecular hydrogen bonds give rise to broad bands, whereas bands arising from intramolecular hydrogen bonds are sharp and well resolved. Other information which can be obtained from the vibrational spectra concerns the strength and the type of O-H···O hydrogen bonds, which remain practically the same in the strongly hydrogen bonded crystals such as KH_2PO_4, NaH_2PO_4, $CsHSO_4$, and CsH_2PO_4 [41-44]. The corresponding OH stretching vibration gives rise to characteristic broad trio bands of ABC type, associated with strongly hydrogen-bonded systems.

These bonds have been interpreted as OH stretching modes in Fermi resonance with combinations involving mainly OH bending vibrations or in terms of a strong coupling between fast OH and O···O stretching modes [45,46]. By knowing the bond length, the strength of the hydrogen bond can be determined as very strong (below 2.5 Å), strong (2.5-2.7 Å), normal (2.7-2.9 Å) and weak (above 2.9 Å). X-ray diffraction analysis of TEAs, reveal that the structure is based on sheets of $H_2AsO_4^-$, H_3AsO_4 tetrahedra bonded together by strong intra-layer O-H···O hydrogen bonds, giving to trimmers. The inspection of the IR spectrum reveals a broad and strong band at 3660 cm^{-1}. We have assigned this band to the stretching mode ν(OH) which is not implied in hydrogen bonding. Two broad and weak bands in IR spectrum located at 3526 and 3440 cm^{-1} are assigned to ν(O-H···O) modes. In Raman spectrum, a broad and weak band at 3244 cm^{-1} is also assigned to ν(O-H···O) stretching modes. The in-plane OH bending mode δOH gives rise to a medium band in infrared spectrum with a counterpart in Raman spectrum at 1244 cm^{-1}. The out-of-plane bending γOH mode appears in the region 900-700 cm^{-1}.

3.3. Calorimetric study

DSC-TG of TEAs was done in air at the rate of 5 °C/min. One more characteristic feature of the room temperature TEAs is its high hygroscopicity (Figure 6-7) which, illustrates the calorimetric (DSC) and thermogravimetric (TGA) results. This compound is stable until 345 K, above this temperature; a loss of weight appears at 369 K of TEAs. It is due to the departure of adsorbed water. The two endothermic peak observed at T = 388 K is attributed to the melting of TEAs.

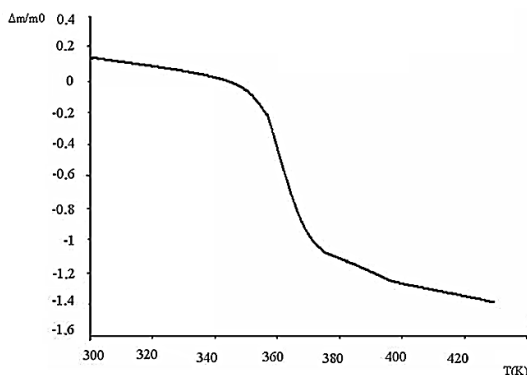**Figure 6.** The TG curve of $[(CH_3CH_2)_4]N$ (H_2AsO_4) $(H_3AsO_4)_2$.
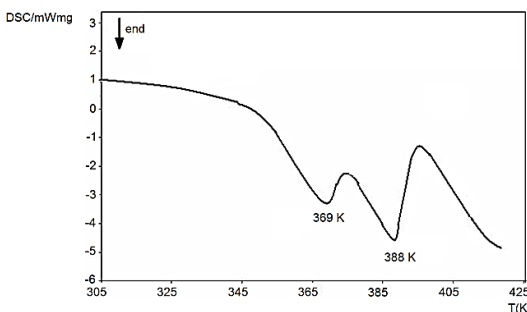
Figure 7. The DSC curve of $[(CH_3CH_2)_4]N$ (H_2AsO_4) $(H_3AsO_4)_2$.

4. Conclusion

The new hybrid material, $[(CH_3CH_2)_4N].[H_2AsO_4].[H_3AsO_4]_2$, has been synthesized and investigated by thermal analysis, single crystal X-ray diffraction and vibrational spectroscopy.

The structure consist of strong two dimensional character based on sheets of $H_2AsO_4^-$ and H_3AsO_4 tetrahedra fused together by strong intra-layer O-H···O hydrogen bonds, giving to trimmers and infinite chains. Vibrational study recorded is of great interest as it verifies the dependence of groups constituting our material. The hydrogen bonds confirmed by IR and X-Ray diffraction explain the stability of our compound. DSC anomalies definitively indicate on adsorbed water and on melting.

Supplementary material

CCDC-927292 contains the supplementary crystallographic data for this paper. These data can be obtained free of charge via www.ccdc.cam.ac.uk/data_request/cif, or by e-mailing data_request@ccdc.cam.ac.uk, or by contacting The Cambridge Crystallographic Data Centre, 12 Union Road, Cambridge CB2 1EZ, UK; fax: +44(0)1223-336033.

References

[1]. Laine, R.; Sanchez , C.; Brinker, C. J.; Gianellis (Eds.), E. Organic/Inorganic Hybrid Materials, Materials Research Society Series, Vol. 628, Pittsburgh, PA. 2000.
[2]. Sanchez, C.; Lebeau, B. *Mater. Res. Soc. Bull.* **2001**, *26*, 377-387.
[3]. Zdanowska-Fraczek, M.; Holderna-Natkaniec, K.; Fraczek, Z. J.; Jakubas, R. *Solid State Ion.* **2009**, *180*, 9-12.
[4]. Chaabane, I.; Hlel, F.; Guidara, K. *J. Alloys Compd.* **2008**, *461*, 495-500.
[5]. Sakai, K.; Takemura, M.; Kawabe, Y. *J. Lumin.* **2010**, *130*, 2505-2507.
[6]. Pradeesha, K.; Sharachandar, Y. G.; Singhb, M.; Vijaya, P. G. *Mater. Chem. Phys.* **2010**, *124*, 44-47.
[7]. Vishwakarma, A.; Ghalsasi, P.; Navamoney, A.; Lan, Y.; Powell, A. *Polyhedron* **2011**, *30*, 1565-1570.
[8]. Aruta, C.; Licci, F.; Zappettini, A.; Bolzoni, F.; Rastelli, F.; Ferro, P.; Bezagni, T. *Appl. Phys. A* **2005**, *81*, 963-968.
[9]. Bujak, M.; Zaleski, J. *Cryst. Eng.* **2001**, *4*, 241-243.
[10]. Karoui, K.; Rhaiem, A. B.; Guidara, K. *Physica B* **2012**, *407*, 489-493.
[11]. Baouab, L.; Jouini, A. *J. Solid State Chem.* **1998**, *141*, 343-351.
[12]. Averbuch-Pouchot, M. T.; Durif, A. *Acta Cryst. C* **1987**, *43*, 1894-1896.
[13]. Averbuch-Pouchot, M. T.; Durif, A.; Guitel, J. C. *Acta Cryst. C* **1988**, *44*, 1968-1972.
[14]. Averbuch-Pouchot, M. T.; Durif, A.; Guitel, J. C. *Acta Cryst. C* **1988**, *44*, 99-102.
[15]. Bagieu-Beucher, M. *Acta Cryst. C* **1990**, *46*, 238-240.
[16]. Averbuch-Pouchot, M. T.; Durif, A.; Guitel, J. C. *Acta Cryst. C* **1989**, *45*, 421-423.
[17]. Baran, J.; Sledz, M.; Drozd, M.; Pietraszko, A.; Haznar, A.; Ratajczak, H. *J. Mol. Struct.* **2000**, *526*, 361-371.
[18]. Amirthaganesan, G.; Kandaswamy, M. A.; Dhandapani, M. *Mater. Chem. Phys.* **2008**, *110*, 328-331.
[19]. Dhouib, I.; Al-Juaid, S.; Mhiri, T.; Elaoud, Z. *Cryst. Struct. Theory Appl.* **2013**, *2*, 8-15.
[20]. Dhouib, I.; Elaoud, Z.; Mhiri, T.; Daoud, A. *J. Chem. Crystallogr.* **2012**, *42*, 5, 513-518.
[21]. Dhouib, I.; Guionneau, P.; Pechev , S.; Mhiri, T.; Elaoud, Z. *Eur. J. Chem.* **2013**, *4(2)*, 117-120.
[22]. Sheldrick, G. M.; SHELX-97, Program for the Solution of Crystal Structures and Crystal Determination, Univ. of Göttingen: Germany, **1997**.
[23]. Baur, W. *Acta Crystallgr. B* **1974**, *30*, 1195-1215.
[24]. Brown, I. D. *Acta Cryst. A* **1976**, *32*, 24-31.
[25]. Blessing, R. H. *Acta Cryst. B* **1986**, *42*, 604-613.
[26]. Nailii, H.; Mhiri, T.; Jaud, J. *J. Solid. State Chem.* **2001**, *161*, 9-16.
[27]. Le Calve, N.; Romain, F.; Limage, M. H.; A. Novak, A. *J. Mol. Struct.* **1989**, *200*, 131-137.
[28]. Hubert, J. I.; Jayakumar, V. S.; Aruldhas, G. *J. Solid State Chem.* **1995**, *120*, 343-347.
[29]. Romain, F.; Novak, A. *J. Mol. Struct.* **1991**, *263*, 69-74.
[30]. Rui-Zhou, Z.; Xiao-Hong, L. Xian-Zhou, Z. *Chin. J. Struct. Chem.* **2012**, *31*, 1395-1408.
[31]. Silverstein, R. M.; Webster, F. X. Spectrometric, Identification of Organic Compounds, Wiley, New York, 1973.
[32]. Gosniowska, M.; Ciunik, Z.; Bator, G.; Jakubas, R.; Baran, J. *J. Mol. Struct.* **2000**, *555*, 243-255.

[33]. Karbowiak, M.; Hanuza, J.; Janczak, J.; Drozdzynski, J. *J. Alloys Compd*. **1995**, *225*, 338-343.
[34]. Karabacak, M.; Cinar, Z.; Kurt, M.; Sudha, S.; Sundaraganesan, N. *Spectrochim. Acta A* **2012**, *85*, 179-189.
[35]. Colthup, N. B.; Daly, L. H.; Wiberley, S. E. Introduction to Infrared and Raman Spectroscopy, Academic Press, New York, 1990.
[36]. Heddrich, H. G.; Blom, C. E. *J. Chem. Phys.* **1989**, *90*, 4660-4663.
[37]. Heddrich, H. G.; Blom, C. E. *J. Mol. Spectrosc*. **1990**, *140*, 103-106.
[38]. Kirkwood, A. D.; Bier, K. D.; Thompson, J. K.; Haslett, T. L.; Hubber, A. S.; Moskovits, M. *J. Phys. Chem*. **1991**, *95*, 2644-2652.
[39]. Edsall, J. T. *J. Chem. Phys.* **1937**, *5*, 225-232.
[40]. Hajlaoui, S.; Chaabane, I.; Oueslati, A.; Guidara, K.; Bulou, A. *Spectrochimi Acta A*. **2014**, *117*, 225-233.
[41]. Marchon B.; Novak, A. *J. Chem. Phys*. **1985**, *78*, 2105-2110.
[42]. Ohno, N.; Lockwood, D. J. *J. Chem*. *Phys*. **1985**, *83*, 4374-3379.
[43]. Choi. B. K.; Kim, J. J. *Jpn. J. Appl. Phys*. **1985**, *24*, 912-914.
[44]. Baran, J. *J. Mol. Struct*. **1987**, *162*, 211-228.
[45]. Hadzi, D.; Bratos, S. The Hydrogen Bond, Vol. 2, North-Holland, Amsterdam, 1976, p. 565.
[46]. Hofacker, G. L.; Marechal, Y.; Ratner, M. A. The Hydrogen Bond, Vol. 1, North-Holland, Amsterdam, 1976, p. 295.